



Numerical Modeling and Computation of Storm Surge for Primitive Equation by Hydrodynamic Model

W. Wannawong[†], U.W. Humphries, P. Wongwiset,
S. Vongvisessomjai and W. Lueangaram

Abstract : The numerical modeling and computation of storm surge in the shallow regions of the South China Sea (SCS) and the Gulf of Thailand (GoT) are important to study the impacts of tropical storms. The storm surge causes the inundation at the lateral boundary exhibiting in the coastal zones of some parts of the SCS and GoT. The predictions of extreme weather events in the SCS and GoT are important to protect the local properties and human life. In the present study, the Princeton Oceanic Model (POM) is used to simulate the tropical storm-induced surge in a case study of Typhoon Linda 1997. The model results compared with the tide gauge station data can describe the characteristics of storm surges at the coastal regions.

Keywords : Gulf of Thailand, hydrodynamic model, South China Sea, storm surge.

2000 Mathematics Subject Classification : 81T80, 91B76, 91B74.

1 Introduction

The model parameters and numerical experiments are designed to study the storm surges by the hydrodynamic model. It is important to solve the governing equation with the surface boundary condition by the numerical modeling.

The governing equation of the Princeton Oceanic Model (POM)[1] describes the Reynold's averaged equations of mass, momentum, temperature and salinity

The authors would like to acknowledge the Commission on Higher Education for giving financial support to Mr.Worachat Wannawong under the Strategic Scholarships Fellowships Frontier Research Networks (CHE-PhD-THA-NEU) in 2007.

Copyright © 2010 by the Mathematical Association of Thailand. All rights reserved.

conservations that are called the primitive equation. The POM model has been developed to study the external gravity waves, internal gravity waves, tidal waves, surges and currents. The model has been used to study currents in the GoT by the Royal Thai Navy since 2000 and it was also developed by the Thailand Research Fund in 2003 in order to study the storm–surge and the effect of tidal forcing. Aschariyaphota et al. [6] studied the seasonal circulations and thermohaline variabilities by using the orthogonal curvilinear grid in the horizontal coordinates and stated that the effects of wind forcing with open boundary condition were important for seasonal circulations. Wannawong et al. [15] studied the comparison of orthogonal curvilinear grid and orthogonal rectangular grid in the horizontal coordinates. Although the orthogonal curvilinear grid provided more acceptable velocity of seawater current in the coastal area than the orthogonal rectangular grid, the velocities of current from both grids were not much different. The orthogonal rectangular grid, therefore, was applied to study the storm surge and current.

The objective of this study is to modify the primitive equation and the surface boundary condition for the storm surge cases. The study domain was extended from the domain used in the report of Wannawong et al. [15] and applied to study the storm surge cases of Typhoon Linda 1997 by the POM model in the present study. The domain covering from $99^{\circ}E$ to $111^{\circ}E$ in longitude and from $2^{\circ}N$ to $14^{\circ}N$ in latitude [16] is applied to three experiments; 2D–barotropic mode, 3D–baroclinic mode in the prognostic option and 3D–baroclinic mode in the diagnostic option. The experiments are calculated in the study domain by the POM model as shown in Figure 1. The outline of this study is organized as follows: Section 2 gives a brief description of the hydrodynamic model and its application to the GoT; Section 3 presents the model parameters and numerical experiments; Section 4 shows the results of experiments; and Section 5 presents the discussions and conclusion.

2 Hydrodynamic Model and Its Application

The numerical model used in the present study has been used operationally in this section. It was developed from the Princeton Oceanic Model (POM) [1] to predict or hindcast surges, inundations, currents and coastal circulations. In this section, a brief description of the model as it is applied in the GoT is given in the following sections.

2.1 The Hydrodynamic Model

The governing equation of the hydrodynamic model can be expressed in the system of orthogonal Cartesian coordinates which consist of the Reynold’s averaged equations of mass, momentum, and temperature and salinity conservations. The equations include the effect of the gravitational/buoyancy forces as well as the effect of the Coriolis pseudo–force which are followed in this section.

Continuity equation:

$$\frac{\partial u}{\partial x} + \frac{\partial v}{\partial y} + \frac{\partial w}{\partial z} = 0, \quad (2.1)$$

x -momentum equation:

$$\frac{\partial u}{\partial t} + \frac{\partial(u^2)}{\partial x} + \frac{\partial(uv)}{\partial y} + \frac{\partial(uw)}{\partial z} = -\frac{1}{\rho_o} \frac{\partial p}{\partial x} + fv + \frac{\partial}{\partial z} \left(A_{mv} \frac{\partial u}{\partial z} \right) + F_x, \quad (2.2)$$

y -momentum equation:

$$\frac{\partial v}{\partial t} + \frac{\partial(uv)}{\partial x} + \frac{\partial(v^2)}{\partial y} + \frac{\partial(vw)}{\partial z} = -\frac{1}{\rho_o} \frac{\partial p}{\partial y} - fu + \frac{\partial}{\partial z} \left(A_{mv} \frac{\partial v}{\partial z} \right) + F_y, \quad (2.3)$$

z -momentum or hydrostatic equation:

$$\frac{\partial p}{\partial z} = -\rho g, \quad (2.4)$$

Temperature equation:

$$\frac{\partial T}{\partial t} + \frac{\partial(uT)}{\partial x} + \frac{\partial(vT)}{\partial y} + \frac{\partial(wT)}{\partial z} = \frac{\partial}{\partial z} \left(A_{hv} \frac{\partial T}{\partial z} \right) + F_T, \quad (2.5)$$

Salinity equation:

$$\frac{\partial S}{\partial t} + \frac{\partial(uS)}{\partial x} + \frac{\partial(vS)}{\partial y} + \frac{\partial(wS)}{\partial z} = \frac{\partial}{\partial z} \left(A_{hv} \frac{\partial S}{\partial z} \right) + F_S, \quad (2.6)$$

The terms F_x , F_y , F_T and F_S found in the equations (2.2), (2.3), (2.5), and (2.6) represent these unresolved processes and in analogy to molecular diffusion can be written as

$$\begin{aligned} F_x &= \frac{\partial}{\partial x} \left[2A_m \frac{\partial u}{\partial x} \right] + \frac{\partial}{\partial y} \left[A_m \left(\frac{\partial u}{\partial y} + \frac{\partial v}{\partial x} \right) \right], \\ F_y &= \frac{\partial}{\partial y} \left[2A_m \frac{\partial v}{\partial y} \right] + \frac{\partial}{\partial x} \left[A_m \left(\frac{\partial u}{\partial y} + \frac{\partial v}{\partial x} \right) \right], \end{aligned}$$

and

$$F_{T,S} = \frac{\partial}{\partial x} A_h \frac{\partial(T,S)}{\partial x} + \frac{\partial}{\partial y} A_h \frac{\partial(T,S)}{\partial y}.$$

where u , v are the horizontal components of the velocity vector ($m s^{-1}$), w is the vertical component of the velocity vector ($m s^{-1}$), g is the gravitational acceleration ($m s^{-2}$), p is the local pressure (Pa), $\rho(x, y, z, t, T, S)$ is the local density ($kg m^{-3}$), ρ_o is the reference water density ($kg m^{-3}$), A_m is the horizontal turbulent diffusion coefficient ($m^2 s^{-1}$), A_{mv} is the vertical turbulent diffusion coefficient ($m^2 s^{-1}$), $f = 2\Omega \sin \phi$ is the Coriolis parameter where Ω is the speed of

angular rotation of the Earth by $\Omega = 7.2921 \times 10^{-5} \text{ rad s}^{-1}$ and ϕ is the latitude ($^{\circ}$ or degree), T is the potential temperature ($^{\circ}\text{C}$), S is the potential salinity (psu), A_h is the horizontal thermal diffusivity coefficient ($\text{m}^2 \text{ s}^{-1}$), A_{hv} is the vertical thermal diffusivity coefficient ($\text{m}^2 \text{ s}^{-1}$), the terms F_x and F_y are the horizontal viscosity terms and the terms F_T and F_S are the horizontal diffusion terms of temperature and salinity respectively.

The main assumptions used in the derivation of the above equations are that: (a) the water is incompressible ($D\rho/Dt = 0$); (b) the density differences are small and can be neglected, except in buoyant forces (Boussinesq approximation). Consequently, the density ρ_o used in the x and y momentum equations (2.2) and (2.3) is a reference density that is either represented by the standard density of the water or by the depth averaged water density as follows:

$$\rho_o = \frac{1}{\eta + h} \int_{-h}^{\eta} \rho dz = \frac{1}{D} \int_{-h}^{\eta} \rho dz \quad (2.7)$$

where the total depth D is expressed as: $D = \eta + h$ that is, the sum of the sea surface elevation η above the mean sea level (MSL) plus the depth h of the still water level. The density ρ used in the z -momentum is represented by the sum of the reference density ρ_o and its variation ρ' ($\rho = \rho_o + \rho'$); and (c) vertical dimensions are much smaller than horizontal dimensions of the water field and vertical motions are much smaller than the horizontal ones. Consequently, the vertical momentum equation reduces to the hydrostatic law (hydrostatic approximation) and the Coriolis term $2\Omega(v \sin \phi - w \cos \phi)$ reduces to $2\Omega v \sin \phi$ (see equation (2.2)). The vertical integration of equation (2.4) from a depth z to the free surface η yields the pressure at water depth z as:

$$p|_{\eta} - p|_z = g \int_z^{\eta} \rho dz' \longrightarrow p = p_{atm} + g\rho_o(\eta - z) + g \int_z^{\eta} \rho' dz' \quad (2.8)$$

where: z' is a dummy variable for integration, η is the sea surface elevation above the mean sea level (MSL), $p|_z = p = p(x, y, z, t)$ and $p|_{\eta} = p_{atm} =$ Standard Atmospheric Pressure.

To close the above system of the continuity and motion equations, it is necessary to state the relationship of the water density, temperature and pressure. This relationship in POM is coded by the following formulation proposed by Mellor [2], that approximates the more general, but also more computationally expensive, formulation of the International Equation of State (UNESCO):

$$\rho(S, T, p) = \rho(S, T, 0) + \frac{p}{c^2} (1 - 0.20 \frac{p}{c^2}) \cdot 10^4 \quad (2.9)$$

$$c(S, T, p) = 1449.2 + 1.34(S - 35) + 4.55T - 0.045T^2 + 0.00821p + 15.0 \cdot 10^{-9}p^2 \quad (2.10)$$

where T is the temperature ($^{\circ}\text{C}$), p is the gage pressure (dbar), S is the salinity (psu) and c is the speed of sound (m s^{-1}).

2.2 Boundary Conditions

Surface boundary conditions:

The continuity, momentum and temperature surface boundary conditions describe the interaction of the water surface with the atmosphere. They are defined as:

$$w|_{\eta} = \left[\frac{\partial \eta}{\partial t} + u \frac{\partial \eta}{\partial x} + v \frac{\partial \eta}{\partial y} \right]_{\eta} \quad (2.11)$$

$$A_{mv} \begin{pmatrix} \partial u / \partial z \\ \partial v / \partial z \end{pmatrix}_{\eta} = \begin{pmatrix} \tau_{sx} / \rho_o \\ \tau_{sy} / \rho_o \end{pmatrix} \quad (2.12)$$

$$\dot{T} = \rho_o A_{hv} \frac{\partial T}{\partial z} \Big|_{\eta} \quad (2.13)$$

$$\dot{S} = \rho_o A_{hv} \frac{\partial S}{\partial z} \Big|_{\eta} \quad (2.14)$$

The equation (2.11) represents the surface boundary condition for the continuity equation (2.1), as expressed by the kinematic free surface condition. At the free surface, the kinematic boundary condition can be derived considering the fact that the free surface is a material boundary for which a particle initially on the boundary will remain on the boundary. Assuming that there is no water penetrating the free surface, then the material or total derivative at the free surface ($\eta - z$) is zero, therefore:

$$\frac{D(\eta - z)}{Dt} = \frac{D\eta}{Dt} - \frac{Dz}{Dt} = 0 \implies \left[\frac{\partial \eta}{\partial t} + u \frac{\partial \eta}{\partial x} + v \frac{\partial \eta}{\partial y} + w \frac{\partial \eta}{\partial z} \right]_{\eta} - \left[\frac{\partial z}{\partial t} + u \frac{\partial z}{\partial x} + v \frac{\partial z}{\partial y} + w \frac{\partial z}{\partial z} \right]_z = 0 \quad (2.15)$$

Since, $\partial \eta / \partial z = \partial z / \partial t = \partial z / \partial x = \partial z / \partial y = 0$ and $\partial z / \partial z = 1$, the equation (2.15) reduces to the equation (2.11).

The equation (2.12) represents the surface boundary condition for the z -momentum or hydrostatic equation (2.4) with the surface wind stresses given by the drag law (bulk formula) as:

$$\begin{pmatrix} \tau_{sx} \\ \tau_{sy} \end{pmatrix} = \rho_{air} C_M W \begin{pmatrix} W_x \\ W_y \end{pmatrix} ; \tau_s = \rho_{air} C_M |W| W ; W = (W_x^2 + W_y^2)^{1/2} \quad (2.16)$$

where W is the wind speed ($m s^{-1}$) at 10 m above the sea water surface, W_x and W_y are the two components of the wind speed vector, ρ_{air} is the density of the air at the standard atmospheric conditions ($kg m^{-3}$), C_M is the bulk momentum transfer (drag) coefficient and τ_s is the wind imposed surface stress.

The drag coefficient (C_M) is assumed to vary with wind speed as:

$$10^3 C_M = \begin{cases} 2.5 & \text{if } |W| > 22 \text{ m s}^{-1} \\ 0.49 + 0.065|W| & \text{if } 8 \leq |W| \leq 22 \text{ m s}^{-1} \\ 1.2 & \text{if } 4 \leq |W| < 8 \text{ m s}^{-1} \\ 1.1 & \text{if } 1 \leq |W| < 4 \text{ m s}^{-1} \\ 2.6 & \text{if } |W| < 1 \text{ m s}^{-1} \\ 0.63 + 0.066|W| & \text{for all } |W| \\ 0.63 + (0.066|W|^2)^{1/2} & \text{for all } |W|. \end{cases}$$

This C_M formula follows Large and Pond [14] when the wind speed is less than 22 m s^{-1} ; otherwise, it is assumed to be a constant as indicated in Powell et al. [4]. The equations (2.13)–(2.14) represent the surface boundary condition for the temperature and salinity equations (2.5)–(2.6). \dot{T} represents the net surface heat flux and $\dot{S} \equiv S(0)[\dot{E} - \dot{P}]/\rho_o$ where $(\dot{E} - \dot{P})$ represents the net evaporation \dot{E} – precipitation \dot{P} fresh water surface mass flux rate and $S(0)$ represents the surface salinity.

Bottom boundary conditions:

$$w|_{-h} = - \left[u \frac{\partial h}{\partial x} + v \frac{\partial h}{\partial y} \right]_{-h} \quad (2.17)$$

$$A_{mv} \begin{pmatrix} \partial u / \partial z \\ \partial v / \partial z \end{pmatrix}_{-h} = \begin{pmatrix} \tau_{bx} / \rho_o \\ \tau_{by} / \rho_o \end{pmatrix} \quad (2.18)$$

$$\rho_o A_{hv} \frac{\partial T}{\partial z} \Big|_{-h} = 0 \quad (2.19)$$

$$\rho_o A_{hv} \frac{\partial S}{\partial z} \Big|_{-h} = 0 \quad (2.20)$$

The equation (2.17) represents the bottom boundary condition for the continuity equation (2.1), as expressed by the kinematic boundary condition. At the bottom, the kinematic boundary condition reflects the fact that there is no flow normal to the boundary, therefore, the material derivative $z + h$ is zero:

$$\begin{aligned} \frac{D(z+h)}{Dt} &= \frac{Dz}{Dt} + \frac{Dh}{Dt} = 0 \implies \\ \left[\frac{\partial z}{\partial t} + u \frac{\partial z}{\partial x} + v \frac{\partial z}{\partial y} + w \frac{\partial z}{\partial z} \right]_{-h} + \left[\frac{\partial h}{\partial t} + u \frac{\partial h}{\partial x} + v \frac{\partial h}{\partial y} + w \frac{\partial h}{\partial z} \right]_{-h} &= 0 \end{aligned} \quad (2.21)$$

and since, $\partial z / \partial t = \partial h / \partial t = \partial z / \partial x = \partial z / \partial y = \partial h / \partial z = 0$ and $\partial z / \partial z = 1$, the equation (2.21) reduces to the equation (2.17).

The equation (2.18) represents the bottom boundary condition for the z -momentum or hydrostatic equation (2.4). The bottom shear stresses are parameterized as follows:

$$\begin{pmatrix} \tau_{bx} \\ \tau_{by} \end{pmatrix} = \rho_o C_D |u| \begin{pmatrix} u \\ v \end{pmatrix} ; \quad \tau_b = \rho_o C_D |u| u ; \quad |u| = (u^2 + v^2)^{1/2} \quad (2.22)$$

where u and v are the horizontal flow velocities at the grid point closest to bottom and C_D is the bottom drag coefficient determined as the maximum between a value calculated according to the logarithmic law of the wall and a value equal to 0.0025:

$$C_D = \max \left[\mathbf{k}^2 \left(\ln \frac{h + z_b}{z_o} \right)^{-2}, 0.0025 \right] \quad (2.23)$$

where z_o is the bottom roughness height in the present application $z_o = 1 \text{ cm}$, z_b is the grid point closest to bottom, and $\mathbf{k} = 0.4$ is the von Kármán's constant. In the 2D barotropic mode of the POM model, C_D is 0.0025.

On the side walls and bottom of the gulf, the normal gradients of T and S in the equations (2.19) and (2.20) are zero. Therefore, there are no advective and diffusive heat and salt fluxes across these boundaries.

Lateral boundary conditions:

The GoT is modeled as a closed gulf without inflow or outflow from the gulf rivers. Consequently, the lateral conditions for a wall boundary are specified such that: (a) there is no flow normal to the wall ($\partial \mathbf{u}_n / \partial n = 0$), and (b) the no slip conditions tangential to the wall are valid ($\mathbf{u}_\tau = 0$), where \mathbf{u} represents the velocity vector, and n and τ are the normal and tangential directions.

2.3 Wind Stress and Atmospheric Pressure Conditions

The typhoon pressure field and surface wind velocity created by the pressure gradient were modeled following the Bowden [3] and Pugh [11] relationships:

$$\frac{\partial p_{air}}{\partial \eta} = -\rho g, \quad (2.24)$$

$$\frac{\partial \eta}{\partial x} = \frac{\rho_{air} C_M W^2}{\rho g D}. \quad (2.25)$$

where p_{air} is the atmospheric pressure (Pa), η is the sea surface elevation (m) from the reference level of undisturbed surface, ρ is the density of sea water ($kg \text{ m}^{-3}$) in the z -momentum, g is the gravitational acceleration of the earth ($m \text{ s}^{-2}$), x is the coordinate in the east-west direction ($^\circ$ or degree), ρ_{air} is the density of air ($kg \text{ m}^{-3}$), C_M is the drag coefficient, W is the wind profile ($m \text{ s}^{-1}$) that results from the typhoon pressure gradient and D is the total depth of sea water (m). According to the equation (2.24), the pressure decreasing for 1 mb corresponds to about a 1 cm rise in sea level. The total water depth D inversely affects the sea surface elevation η , whereas the wind speed at the specific height (10 m) directly affects the sea surface elevation.

2.4 Stability Condition

The Courant–Friedrichs–Lewy (CFL) computational stability condition on the external and internal modes are described below:

$$\Delta t_E \leq \frac{1}{C_t} \left| \frac{1}{\delta x^2} + \frac{1}{\delta y^2} \right|^{-1/2}, \quad (2.26)$$

$$\Delta t_I \leq \frac{1}{C_T} \left| \frac{1}{\delta x^2} + \frac{1}{\delta y^2} \right|^{-1/2}. \quad (2.27)$$

where

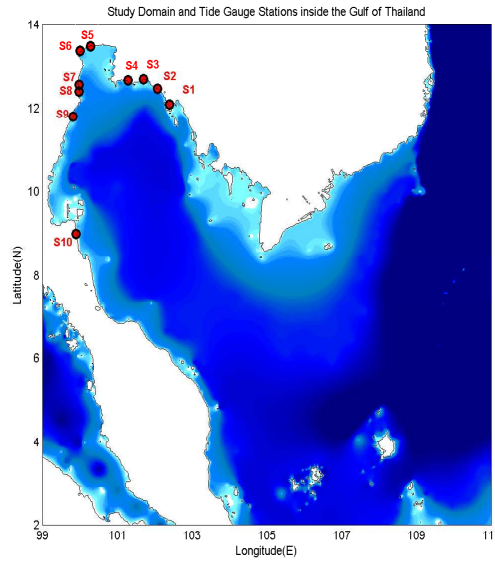
$$\begin{aligned} C_t &= 2(gh)^{1/2} + U1_{max}, \\ C_T &= 2C + U2_{max}. \end{aligned}$$

where Δt_E and Δt_I are the limited time step for the external and internal modes (s), $U1_{max}$ and $U2_{max}$ are denoted as the expected maximum velocity ($m s^{-1}$) and the maximum advective speed ($m s^{-1}$), δx and δy are the grid spacing in x - and y - directions (m), g is the gravitational acceleration of the earth ($m s^{-2}$), h is the depth of the still water level (m) and C is the maximum internal gravity wave speed based on the gravest mode, commonly of order $2 m s^{-1}$. For more details of the sensitivity of the POM model to the time steps, see Ezer et al. [12].

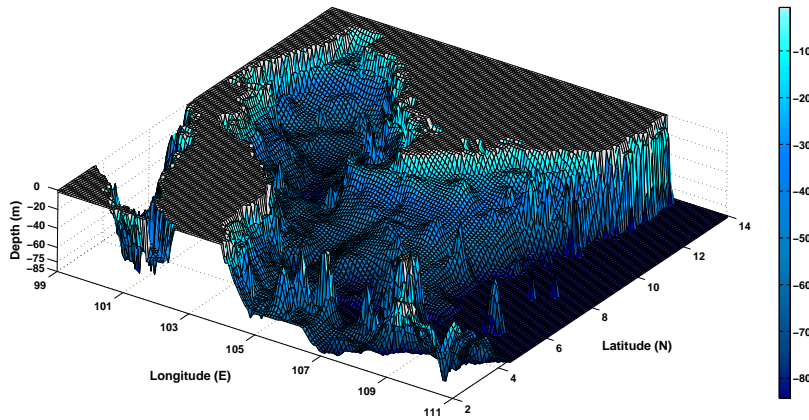
3 Model Parameters and Numerical Experiments

3.1 The Geometry of the Study Domain

The geometry of the study domain is defined by the shoreline, bathymetry and specified transfer boundaries. For the model run in some parts of the SCS and GoT, computations take place on a $0.1^\circ \times 0.1^\circ$ rectilinear horizontal grid and on a sigma vertical grid with 21 layers. The domain covered from $99^\circ E$ to $111^\circ E$ in longitude and from $2^\circ N$ to $14^\circ N$ in latitude. The shoreline and the bathymetry of the GoT on the $0.1^\circ \times 0.1^\circ$ grid were obtained from GEODAS (available online from <http://www.ngdc.noaa.gov/mgg/gdas>) (Figure 1). The original version (1993), ETOPO5 [5], on a 5-minute latitude/longitude grid (1 minute of latitude = 1 nautical mile, or 1.853 km) was updated in June 2005 for the acceptably deep water.



(a)



(b)

Figure 1: (a) The study domain and observational positions and (b) the three dimensional perspective view of topography (in meters).

3.2 Model Initialization and Forcing

The model is initialized by setting the velocity, temperature and salinity fields equal to zero. The above set up known as “cold start” requires the model run for spin up period before it reaches a state of statistical equilibrium. In the present application, a typhoon spin up period was adequate for the model to reach equilibrium and to provide realistic results.

The forcing of model during the spin up period and the subsequent model simulations require the use of the following meteorological data: temperature, salinity, sea level pressure, wind speed and direction. The wind and pressure fields were obtained from the U.S. Navy Global Atmospheric Prediction System (NOGAPS) which is a global atmospheric forecast model with $1^\circ \times 1^\circ$ data resolution (Hogan and Rosmond [13]; Harr et al. [7]). The temperature and salinity with $1^\circ \times 1^\circ$ data resolution provided by Levitus94 (Levitus and Boyer [9]; Levitus et al. [8]) were indicated by the climatological monthly mean fields in the model. The high resolution of $0.1^\circ \times 0.1^\circ$ spatial grid size gave 121×121 points by using the bilinear interpolation of these data in the horizontal coordinate. In the vertical coordinate, 21 sigma levels were employed for adequacy and computational efficiency. The model time steps were 20 s and 1200 s (20 min) for the external and internal time steps respectively.

The horizontal momentum equations consist of the local time derivative and horizontal advection terms, Coriolis deflection, sea level pressure gradient, tangential wind stress on the sea surface, and quadratic bottom friction. The system of equations is written in the flux form and solved by using the finite differential method that is centered in time and space on the Arakawa C grid. Finally, the results of the POM model were correspondingly represented in every hour of Typhoon Linda 1997 passing in some parts of the SCS and GoT. The stability of the model was computed according to the CFL stability condition.

3.3 Experimental Designs

In order to compute the storm surge on the sea surface layer, three experiments were performed (Table 1). The hydrodynamic model used in this study was the POM model including the storm surge applications. The POM model was run by considering the difference between 2D and 3D modes. The model simulations were conducted utilizing the 2D mode of the POM model as the primary objectives were to study the barotropic water level variation and volume exchange. To test the adequacy of the POM model, the 2D and 3D modes were tested as described above.

4 Results of Experiments

The simulations of storm surge were analyzed from a set of model experiments: Exp.I, Exp.II and Exp.III as described in Table 1.

Table 1: The description and reference codes of the numerical experiments

Experimental code	Description of numerical experiments
Exp.I	2D–barotropic mode
Exp.II	3D–baroclinic mode in the prognostic option
Exp.III	3D–baroclinic mode in the diagnostic option

The storm surge generated by Typhoon Linda was firstly considered (Exp.I) and computed by using the POM model (Figure 3). The Bowden [3] and Pugh [11] relationships have been used to describe the storm surges related with the strong wind and low pressure (Figures 2–5). The POM model using in the three experiments was run with the same wind field (wind speed), pressure field (sea level pressure), domain (wind fetch) and also the same time (duration) but with the different computational options. Figures 4(a) and (b) showed the storm surges at the same location and time with the different optional calculation in Exp.II. In Exp.III, the difference of optional calculation on the sea surface layer can be easily considered in Figures 3–5, which showed that the storm surge increased the setup and slowed down the difference of water recession in 2D and 3D calculations.

The effects of extreme of storm surge and the difference between the maximum storm surges computed by the POM model at ten locations of the tide gauge station at border of the GoT region (Figure 1(a) and Table 2) were calculated. The differences of storm surges at each station were presented in Table 3. The results showed that the maximum storm surges of all experiments at each station presented the similar values and also showed the similar trends with the observational data, except those of stations S5, S6 and S8.

Table 2: The computational and observational points for the hydrodynamic model simulations

Station code	Station name	Station point	Computational point
S1	Laem Ngob	102.40° E 12.10° N	102.38° E 12.08° N
S2	Laem Sing	102.07° E 12.47° N	102.05° E 12.47° N
S3	Prasae	101.70° E 12.70° N	101.70° E 12.68° N
S4	Rayong	101.28° E 12.67° N	101.28° E 12.65° N
S5	Tha Chin	100.28° E 13.48° N	100.28° E 13.45° N
S6	Mae Klong	100.00° E 13.38° N	100.03° E 13.35° N
S7	Pranburi	99.98° E 12.40° N	100.10° E 12.40° N
S8	Hua Hin	99.97° E 12.57° N	99.95° E 12.57° N
S9	Ko Lak	99.82° E 11.80° N	99.84° E 11.78° N
S10	Sichol	99.90° E 9.00° N	99.92° E 8.98° N

Table 3: The comparisons of the maximum storm surges of the hydrodynamic model with the observational data

Station code	Station name	Exp.I (m)	Exp.II (m)	Exp.III (m)	Obs. (m)
S1	Laem Ngob	0.24272	0.29315	0.3946	1.18
S2	Laem Sing	0.27754	0.34295	0.4506	1.23
S3	Prasae	0.29275	0.36319	0.47255	1.34
S4	Rayong	0.33268	0.40797	0.52016	1.18
S5	Tha Chin	0.43644	0.52228	0.64734	2.08
S6	Mae Klong	0.459	0.551	0.68793	1.96
S7	Pranburi	0.43598	0.52042	0.6417	1.44
S8	Hua Hin	0.45163	0.53971	0.66103	2.46
S9	Ko Lak	0.37148	0.43224	0.52886	1.32
S10	Sichol	0.23824	0.35712	0.41345	1.1

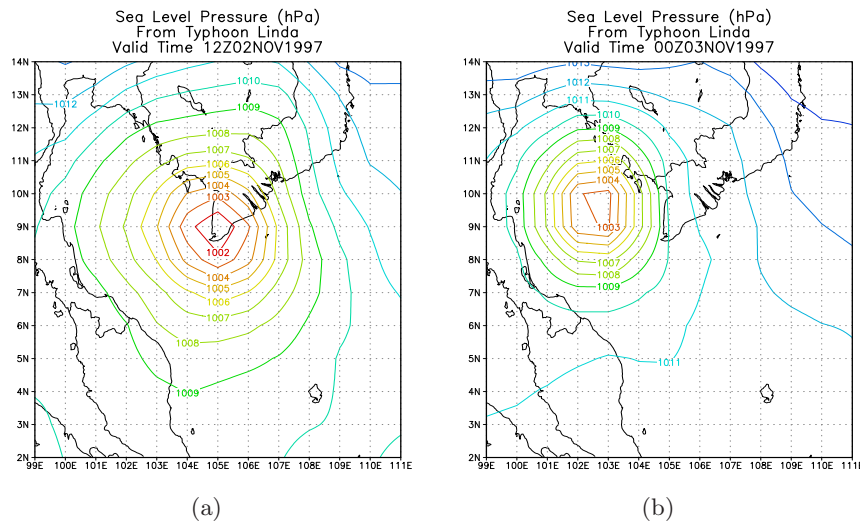


Figure 2: The sea level pressure at the sea surface layer (a) before and (b) after entering into the GoT

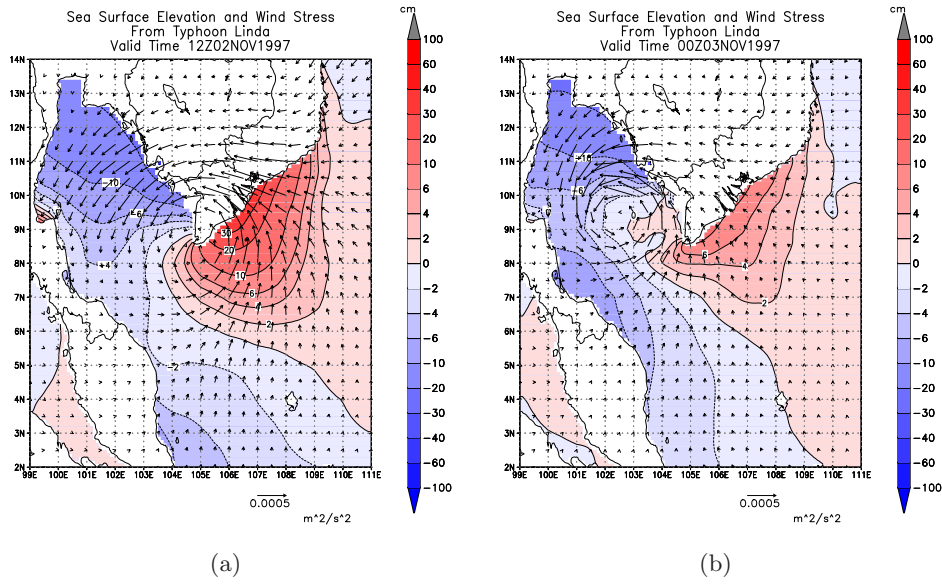


Figure 3: The sea surface elevation and wind stress in the 2D-barotropic mode (a) before and (b) after entering into the GoT

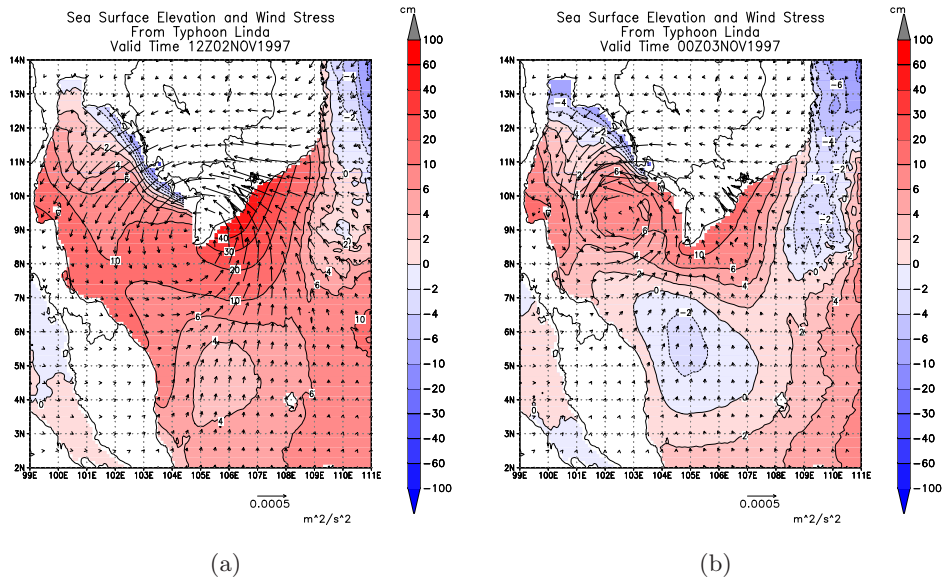


Figure 4: The sea surface elevation and wind stress in the 3D-baroclinic mode with the prognostic option (a) before and (b) after entering into the GoT

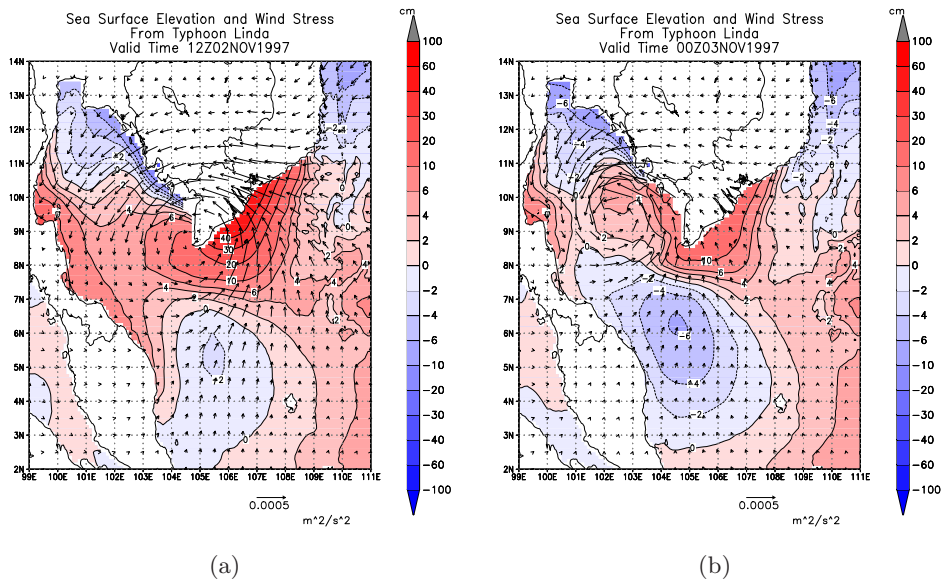


Figure 5: The sea surface elevation and wind stress in the 3D–baroclinic mode with the diagnostic option (a) before and (b) after entering into the GoT

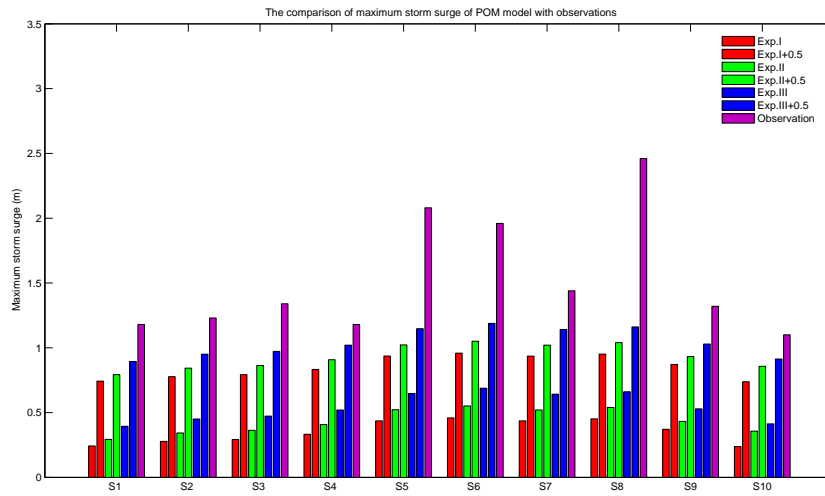


Figure 6: The comparisons of the maximum storm surges at each station

5 Discussions and Conclusion

The comparisons of storm surges on the sea surface layer of the three experiments (Figure 6 and Table 3) in Typhoon Linda case revealed that the storm surge played a more significant role in determining the computations for the primitive equation by the hydrodynamic model (POM model). The role of storm surge with the included assumption of tide forcing ± 0.5 m can be clearly considered in Figure 6. The slight differences of storm surges between Exp.I, Exp.II, Exp.III and the observational data with typhoon distribution during Typhoon Linda entering into the GoT are shown in Figure 6 and Table 3.

The results of model can be considered that the 3D–baroclinic mode increased the setup and slowed down the water recession, thus improving the model performance during the water level declining period while over predicted surge during the water level rising period. Since the specification of the bottom boundary condition depends on the assumption of the vertical velocity profile, the treatments of boundary condition in 2D and 3D modes are not identified, which resulted in the slight different results. The results indicated that the 3D mode did not produce better results compared to the baseline simulation without additional calibration of the 3D mode case, but the differences are not significant.

For the vertically integrated sea surface elevation calculated by the POM model, the numerical experiments involving the use of the storm surge model in the prognostic and diagnostic modes in the 3D mode have been performed. In the prognostic mode, the momentum equations as well as the temperature and salinity distributions of the governing equation were integrated as an initial value problem. These predictive experiments do not always reach steady state since the oceanic response time for the density field can be considerable. As an alternative, diagnostic computation was considered. Additional studies will be investigated in the future with a focus on how storm surges affect other domains in the GoT. The effects of storm surge on the sea surface layer should be more comprehensively examined with more typhoon case simulations. Additionally, the observational data are needed to calibrate and validate with the harmonic analysis of tide in other models (Vongvisessomjai et al. [10]).

Acknowledgements. The authors would like to acknowledge the Commission on Higher Education for kindly providing financial support to Mr. Worachat Wannawong under the Strategic Scholarships Fellowships Frontier Research Networks (CHE–PhD–THA–NEU) in 2007. We wish to thank the Geo–Informatics and Space Technology Development Agency (Public Organization) (GISTDA) for buoy data and documents. We are grateful to the Meteorological Division, Hydrographic Department, Royal Thai Navy, Sattahip, Chonburi, Thailand, for kindly providing the laboratory space. Finally, the helpful comments on English grammar and usage of Mr. Michael Willing is also gratefully acknowledged.

References

- [1] A. F. Blumberg and G. L. Mellor, A description of a threedimensional coastal ocean circulation model, In N. S. Heaps, editor, Three-dimensional coastal ocean models, Coastal and estuarine sciences 4, American Geophysical Union, (1987), 1–16.
- [2] G. L. Mellor, An Equation of State for Numerical Models of Oceans and Estuaries, *Journal of Atmospheric and Oceanic Technology*, 8(1991), 609–611.
- [3] K. F. Bowden, *Physical Oceanography of Coastal Waters*, Ellis Horwood, Southampton, UK., (1983), 302.
- [4] M. D. Powell, P. J. Vivkery and T. A. Reinhold, Reduced drag coefficient for high wind speeds in tropical cyclones, *Nature*, 422(2003), 278–283.
- [5] M. O. Edwards, Global Gridded Elevation and Bathymetry on 5–Minute Geographic Grid (ETOPO5), NOAA, National Geophysical Data Center, Boulder, Colorado, U.S.A., 1989.
- [6] N. Ascharyaphotha, P. Wongwises, S. Wongwises, U. W. Humphries and X. You, Simulation of seasonal circulations and thermohaline variabilities in the Gulf of Thailand, *Advances in Atmospheric Sciences*, 25(2008), 489–506.
- [7] P. Harr, R. Ellsberry, T. Hogan and W. Clune, North Pacific cyclone sea-level pressure errors with NOGAPS, *Weather and Forecasting*, 7(1992), 3.
- [8] S. Levitus, R. Burgett and T. Boyer, *World Ocean Atlas: Salinity*, NOAA Atlas NESDIS 3, U. S. Government Printing Office, Washington D.C., U.S.A., 3(1994b), 99.
- [9] S. Levitus and T. Boyer, *World Ocean Atlas: Temperature*, NOAA Atlas NESDIS 4, U. S. Government Printing Office, Washington D.C., U.S.A., 4(1994a), 117.
- [10] S. Vongvisessomjai, P. Chatanantavet and P. Srivihok, Interaction of tide and salinity barrier: Limitation of numerical model, *Songklanakarin Journal of Science and Technology*, 30(2008), 531–538.
- [11] T. D. Pugh, *Tides, Surges and Mean Sea-Level*, John Wiley & Sons, London, UK., (1987), 472.
- [12] T. Ezer, H. Arango and A. F. Shchepetkin, Developments in terrain-following ocean models: intercomparison of numerical aspects, *Ocean Modelling*, 4(2002), 249–267.
- [13] T. F. Hogan and T. E. Rosmond, The description of the Navy Operational Global Atmospheric System’s spectral forecast model, *Monthly Weather Review*, 119(1991), 1786–1815.

- [14] W. G. Large and S. Pond, Open ocean momentum fluxes in moderate to strong winds, *Journal of Physical Oceanography*, 11(1981), 324–336.
- [15] W. Wannawong, U. W. Humphries and A. Luadsong, The application of curvilinear coordinate for primitive equation in the Gulf of Thailand, *Thai Journal of Mathematics*, 6(2008), 89–108.
- [16] W. Wannawong, U. W. Humphries, P. Wongwises, S. Vongvisessomjai and W. Lueangaram, A numerical study of two coordinates for energy balance equations by wave model, *Thai Journal of Mathematics*, 8(2010), 197–214.

(Received 5 December 209)

W. Wannawong and U.W. Humphries
Department of Mathematics
Faculty of Science
King Mongkut's University of Technology Thonburi
Bangkok 10140, THAILAND.
e-mail: worachataj@hotmail.com and usa.wan@kmutt.ac.th

P. Wongwises
The Joint Graduate School of Energy and Environment
King Mongkut's University of Technology Thonburi
Bangkok 10140, THAILAND.
e-mail: prungchan.won@kmutt.ac.th

S. Vongvisessomjai
Water and Environment Expert
TEAM Consulting Engineering and Management Co., Ltd.
151 TEAM Building Nuan Chan Road, Klong Kum, Bueng Kum
Bangkok 10230, THAILAND.
e-mail: suphat@team.co.th

W. Lueangaram
Meteorological Division, Hydrographic Department
Royal Thai Navy, Sattahip
Chonburi 20180, THAILAND.
e-mail: viriya.navy@gmail.com